1.0

1.1

1.25 1.4 1.6

2.8 2.5

2.2

2.0

1.8

MICROCOPY RESOLUTION TEST CHART

COMPUTATION OF ACOUSTIC POWER, VIBRATION RESPONSE
AND ACOUSTIC PRESSURES OF FLUID-FILLED PIPES

BY

J H JAMES

Summary

The time-harmonic excitation is either an interior point source of sound or a mechanical point force located on the pipe's surface. The acoustic power radiated into the exterior fluid, the vibration response of the pipe's wall, and the pressures in the exterior and interior fluids are computed by a simple integration scheme. Numerical results are presented for the case of a water-filled steel pipe that is surrounded by air.

AMTE (Teddington)
Queens Road
TEDDINGTON Middlesex TW11 OLN

May 1982

C

Copyright
Controller HMSO London
1982

pages 26
figures 9

- 1 -

DTIC
COPY
INSPECTED

LIST OF SYMBOLS

(x,y,z)	= cartesian coordinates
$(r,\emptyset,z)$	= cylindrical coordinates
$(R,\theta,\emptyset)$	= spherical coordinates
$U(\emptyset,z), V(\emptyset,z), W(\emptyset,z)$	= axial, tangential and radial displacements at shell mid-surface
α, n	= axial and circumferential harmonic wavenumbers
$\overline{U}(n,\alpha), \overline{V}(n,\alpha), \overline{W}(n,\alpha)$	= transforms of shell displacements
$p_1(r,\theta,z), p_2(r,\theta,z)$	= interior and exterior pressures
ω	= radian frequency of vibration
ρ_1, c_1	= density and sound velocity of interior fluid
ρ_2, c_2	= density and sound velocity of exterior fluid
k_i, $i=1,2$	= wavenumber in fluid, ω/c_i
a, h, ρ_s	= radius, thickness and density of pipe
E_1	= $Eh/(1-\sigma^2)$. E is Young's modulus and σ is Poisson's ratio
β^2	= $h^2/12a^2$
δ	= Dirac delta function
e_n	= 1 when $n=0$, and 2 otherwise
F_0	= amplitude of point force located at cylindrical coordinates $(a,0,0)$
P_0	= amplitude of point source located at cylindrical coordinates $(X_0,0,0)$
R_0^2	= $(X-X_0)^2 + Y^2 + Z^2 = r^2 + X_0^2 - 2rX_0 \cos(\emptyset) + Z^2$
$J_n, J_n', Y_n, Y_n', H_n H_n'$	= Bessel functions and their derivatives. $H_n = J_n + iY_n$
μ_i, $i=1,2$	= $(k_i^2 - \alpha^2)^{\frac{1}{2}}$ with Im.$(\mu_i) > 0$ to satisfy the radiation condition
η	= hysteretic loss factor of shell

INTRODUCTION

A previous report [1] has analysed the theoretical problem of far-field
sound radiation from fluid-filled pipes that are excited by point forces and
point acoustic sources. The salient points that emerge from the work are
that the frequencies at which 'peaks' appear in the sound spectra depend on
the location of the observation point, and that the far-field radiation
characteristics are understood better when wavenumber versus frequency
dispersion plots are available. In practice, however, measurements in the
far-field are not usually possible because the environment is inevitably
reverberant. It is thus necessary to average spatially the pressure
measurements, in a suitable way, to give an estimate of the radiated
acoustic power. Other responses of central interest to an experimentally
based programme are the pressure fields near to the pipe's surface and the
acceleration response of the pipe's wall.

In Section 2, the pressure fields and the pipe's displacements are
represented by Fourier transforms, and the acoustic power in the surrounding
fluid is obtained from the stationary phase approximation to the far-field
pressure. The integral representations of the fluid pressures, pipe's dis-
placements and radiated power are evaluated by a simple numerical quadrature
scheme. In Section 3, numerical results are discussed for the case of a
water-filled steel pipe that is radiating into the surrounding air. The
numerical results are in the form of decibel level versus frequency plots
for the responses in the individual circumferential harmonics, n=0, 1 and 2.

The numerical results are better understood by inspection of wavenumber
versus frequency plots, but further numerical work is necessary. First, it
is necessary to search the literature for measurements that have been
obtained under controlled conditions, because a comparison with theoretical
estimates would be particularly valuable. Secondly, plots of acoustic
intensity vectors [6] would help to illustrate the essential physics of the
fluid-pipe system. Thirdly, the eigenvectors should help to explain the
curious maxima and minima that appear in the spectra of the responses at a
distance from the source. Forthly, the range of applicability of the
concept of matching wavenumbers of in-vacuo pipe and rigid-walled duct needs
to be investigated in some detail because it is being used increasingly to
explain certain aspects of measured data. Finally, the effect of fluid flow
on the stability, vibration and sound radiation needs to be investigated.

2. PROBLEM FORMULATION

General

An infinite circular thin-walled pipe contains and is also
surrounded by fluids of possibly differing densities and sound veloci-
ties. The displacements of the pipe's wall satisfy an eighth-order
shell theory [2], and the interior and exterior sound pressures satisfy
the Helmholtz wave-equation. The pipe is excited by time-harmonic
surface stresses caused by mechanical point forces or interior acoustic
sources. The time factor exp(-iωt) is omitted from all of the
equations. The geometry is shown in Figure 1.

Pipe Displacements and Fluid Pressures

The axial, tangential and radial displacements of the pipe's wall and the interior and exterior acoustic pressures have the following Fourier transform representations:

$$
\begin{bmatrix} U(\emptyset,z) \\ V(\emptyset,z) \\ W(\emptyset,z) \end{bmatrix} = (1/2\pi) \sum_{n=0}^{\infty} \begin{bmatrix} \cos(n\emptyset) \\ \sin(n\emptyset) \\ \cos(n\emptyset) \end{bmatrix} \int_{-\infty}^{\infty} \exp(i\alpha z) \begin{bmatrix} \overline{U}(n,\alpha) \\ \overline{V}(n,\alpha) \\ \overline{W}(n,\alpha) \end{bmatrix} d\alpha \qquad (2.1)
$$

$$
p_1(r,\emptyset,z) = (1/2\pi) \sum_{n=0}^{\infty} \cos(n\emptyset) \int_{-\infty}^{\infty} \exp(i\alpha z) \, \overline{p}_1(r,n,\alpha) d\alpha \qquad (2.2)
$$

$$
p_2(r,\emptyset,z) = (\omega^2 \rho_2/2\pi) \sum_{n=0}^{\infty} \cos(n\emptyset) \int_{-\infty}^{\infty} \exp(i\alpha z)[H_n(\mu_2 r)/\mu_2 H_n'(\mu_2 a)]
$$
$$
\overline{W}(n,\alpha) d\alpha \qquad (2.3)
$$

Formulae for the transforms $\overline{U}(n,\alpha)$, $\overline{V}(n,\alpha)$, $\overline{W}(n,\alpha)$ and $\overline{p}_1(r,n,\alpha)$ are to be found in the Appendix.

Far-Field Acoustic Pressure

A stationary phase evaluation of the integral representation of the exterior pressure yields the far-field pressure as

$$
p_f(R,\theta,\emptyset) = -i\omega\rho_2 c_2 . \exp(ik_2 R)/\pi R . \sum_{n=0}^{\infty} \frac{\overline{W}(n,k_2\cos\theta)\exp(-in\pi/2).\cos(n\emptyset)}{\sin(\theta)H_n'(ak_2\sin\theta)} \qquad (2.4)
$$

Radiated Power

The acoustic power radiated into the exterior fluid is defined as

$$
P = \int_0^{\pi} \int_0^{2\pi} [\,|p_f(R,\theta,\emptyset)|^2/\rho_2 c_2]\, R^2\sin(\theta) d\theta d\emptyset \qquad (2.5)
$$

where the customary multiplication factor of one-half has been omitted because the excitation is to be specified in its rms form. Substituting equation (2.4) into equation (2.5) gives, after carrying out the integration in the $\emptyset$-coordinate,

$$
P = (2\omega^2\rho_2 c_2/\pi) \sum_{n=0}^{\infty} e_n^{-1} \int_0^{\pi} [\,|\overline{W}(n,k_2\cos\theta)|^2/\sin(\theta)|H_n'(ak_2\sin\theta)|^2]\, d\theta \qquad (2.6)
$$

When the excitation is located at $z=0$, the symmetry of the sound field about $\theta=\pi/2$ may be used to halve the computational time.

Numerical Evaluation of Integrals

The integrals in equations (2.1-2.3) and (2.6) must be evaluated numerically because closed-form expressions are not available. Their numerical approximation, on truncating the infinite limits in equations (2.1-2.3) to finite values, is based upon a simple adaptive quadrature scheme that has been used successfully to evaluate the response and acoustic field of a point-excited plate [3].

The scheme splits the range of integration into a selected number of equal intervals each of which being repeatedly halved until an absolute or a relative convergence test is met by successive approximations to the integral in the interval - Gaussian quadrature of order two is suitable for those cases where low accuracy is sufficient. Vogel & Feit [4] have also used an adaptive scheme to evaluate the vibration response of a pipe with exterior fluid loading and point force excitation - their mesh size being controlled by the second derivative of the integrand.

3. NUMERICAL EXAMPLES

General

Plots of wavenumber, acoustic power, acceleration and acoustic pressure versus frequency are shown in Figures 2-9 for the particular case of a water-filled steel pipe that is surrounded by air. The material and geometric constants, in SI units, used in the computations are as follows:

pipe: $E=19.5E10$, $\sigma=0.29$, $\rho=7700.0$, $h=2.54E-2$, $a=22.23E-2$, $\eta=0.02$

water: $\rho=1000.0$, $c=1500.0$

air: $\rho=1.21$, $c=343.0$

Previous work [1] has presented plots of far-field acoustic radiation versus frequency, for the various combinations of the fluids, air and water, and the separate cases of point force and source excitation.

Wavenumber Plots

Figures 2 and 3 show the real branches of the wavenumber versus frequency plots for the circumferential harmonics $n=0-2$. The loading caused by the surrounding air was neglected. The frequency range extends to 1.4 times the 'ring' frequency of the pipe. The physical interpretation of wavenumber-frequency plots is discussed in some detail elsewhere [5]; here, only a brief explanation of the 'cut-on' nature of the waves is necessary.

Figure 2 contains the plots for a water-filled pipe. First, for $n=0$, the branches labelled 1-4 are close to a plane fluid wave, an axial wave in the pipe, a radial flexural wave in the pipe and a fluid wave, respectively; the branch 'O' is a wave of pure torsion. Secondly, for $n=1$, the branches are the familiar beam flexural wave, a fluid wave and a pipe torsional wave, respectively. Finally, for $n=2$, the branches are the radial shell flexural wave, a fluid wave and a torsional wave, respectively.

- 7 -

Figure 3 contains the wavenumber versus frequency plots for the separate cases of the pipe in-vacuo, a rigid-walled waveguide of water and a pressure release waveguide of water. These plots, when compared with Figure 2, show the effect of the interior water on the real branches of the dispersion relation. They are also useful if the concept of equal wavenumber in the fluid and pipe is of value to the interpretation of the responses of the coupled fluid-pipe system.

Airborne Acoustic Power

Figures 4-5 show the airborne acoustic power radiated from the pipe's wall in the $n=0-2$ circumferential harmonics, for the separate cases of point-source and point-force excitation. The sound power decibel level is defined as $10.\log(P) + 120$.

In Figure 4, the excitation is a point source, located at the cylindrical coordinates $(2a/3,0,0)$, whose free-field level in the interior fluid is 120 dB ref 1 micropascal at 1m. The 'peaks' in the spectra occur at the frequencies at which wave-branches 'cut-on'. In particular, a large jump in the acoustic power occurs at the frequency of the $n=2$ harmonic where an essentially fluid-type wave 'cuts-on'. At frequencies below the 'cut-on' frequency of the $n=2$ flexural mode, the total power is dominated by the contribution of the $n=0$ harmonic.

In Figure 5, the excitation is a radial 1 N point force that is located at the cylindrical coordinates $(a,0,0)$. Again, the peaks in the spectra occur at frequencies at which the wave-branches 'cut-on'. However, the jump in level at the 'cut-on' frequency of the $n=2$ fluid-type wave is less severe, and the radiated power of the $n=0$ harmonic goes to zero at low frequencies where the $n=1$ harmonic is dominant.

The effect, on the power radiation, of additional damping in the pipe's wall was investigated by increasing the hysteretic loss factor from 0.02 to 0.10. The power levels dropped by 7 dB which indicates a power reduction of $10.\log(n_2/n_1)$. It must be borne in mind that this power reduction would not necessarily have been obtained for the case of a water-filled pipe radiating into water, because the radiation loss factor could be of the same order of magnitude as the structural loss factor.

Radial Acceleration of Pipe's Wall

The radial acceleration of the pipe's wall in the $n=0-2$ harmonics is plotted in Figures 6-7 for the case of point force excitation located at $(a,0,0)$. The acceleration decibel levels are defined as $20.\log(|\ddot{W}|) + 100$.

Figure 6 gives the drive point acceleration. It is evident that the maximum responses occur at the 'cut-on' frequencies of the modes. The plots, on adjustment to velocity response, are of similar appearance to the power radiation plots of Figure 5.

Figure 7 gives the acceleration response at an axial distance of 4m from the radial drive force. The responses are now quite complex at the higher frequencies, presumably due to modal interference effects and the changing nature of the wave-branches with frequency [5]. It

- 8 -

is difficult to interpret these plots without the availability of the eigenvectors.

Acoustic Pressures on Pipe's Surfaces

Figures 8-9 show the acoustic pressures on the pipe's outer and inner surfaces, respectively. The excitation is a radial point force and the pressures are computed at an axial distance of 4m from the force, the decibel level being $20.\log(|p|) + 120$.

The plots of the pressure on the outside of the pipe, Figure 8, are of similar appearance to the transfer acceleration, Figure 7. At the higher frequencies, the maxima and minima in the plots of the inside pressure, Figure 9, do not coincide in frequency with those of the outer pressure plots. Indeed, it is curious that many maxima and minima are reversed in the two figures.

4. ACKNOWLEDGEMENT

Thanks are due to E J Clement for his help with the graphical presentations.

J.H. James (PSO)

JHJ/jms

REFERENCES

1. JAMES, J.H., Sound Radiation from Fluid-Filled Pipes, Admiralty Marine Technology Establishment, Teddington, AMTE(N) TM81048, September 1981

2. LEISSA, A.W., Vibration of Shells, NASA SP-288, 1973.

3. MELOTTE, J.A., SPICER, W.J., unpublished work at AMTE (Teddington) on the vibration and sound radiation of point excited plates.

4. VOGEL, W., FEIT, D., Response of a Point Excited Infinitely-long Shell Immersed in an Acoustic Fluid, DTNSRDC(Bethesda), Report 80/061, November 1980.

5. FULLER, C.R., FAHY, F.G., Characteristics of Wave Propagation and Energy Distribution in Cylindrical Elastic Shells Filled with Fluid, Institute of Sound and Vibration Research, Southampton, Contract Report No 81/10, March 1981.

6. SPICER, W.J., Acoustic Intensity Vectors from an Infinite Plate with Line Attachments, Admiralty Marine Technology Establishment, Teddington, AMTE(N) TM81086, October 1981.

A P P E N D I X

The Spectral Displacements [1]

The excitation is either a radial point force, of magnitude F_0, that is located at the cylindrical coordinate $(a,0,0)$, or it is an interior point source of sound, of free-field pressure $p_0 \exp(ik_1 R_0)/R_0$, that is located at $(x_0,0,0)$. The 'spectral' displacements are obtained, via Novozhilov shell theory [2], as the solution of the matrix equation

$$
\begin{bmatrix}
S_{11} & S_{12} & S_{13} \\[4pt]
S_{21} & S_{22} & S_{23} \\[4pt]
S_{31} & S_{32} & S_{33}+\rho_2\omega^2 H_n(\mu_2 a)/\mu_2 H_n'(\mu_2 a) \\[4pt]
 & & -\rho_1\omega^2 J_n(\mu_1 a)/\mu_1 J_n'(\mu_1 a)
\end{bmatrix}
\begin{bmatrix}
\overline{U}(n,\alpha) \\[4pt]
\overline{V}(n,\alpha) \\[4pt]
\overline{W}(n,\alpha)
\end{bmatrix}
=
\begin{bmatrix}
0 \\[4pt]
0 \\[4pt]
F_0 e_n/2\pi a \quad \underline{or} \\[4pt]
2p_0 e_n J_n(\mu_1 x_0)/\mu_1 a J_n'(\mu_1 a)
\end{bmatrix}
\quad \text{(A1)}
$$

where

$$S_{11} = E_1[\alpha^2 + n^2(1-\sigma)/2a^2] - \rho_s h\omega^2$$

$$S_{12} = -E_1 i\alpha n(1+\sigma)/2a$$

$$S_{13} = -E_1 i\alpha\sigma/a$$

$$S_{21} = -S_{12}$$

$$S_{22} = E_1[\alpha^2(1-\sigma)/2 + n^2/a^2 + 2\alpha^2\beta^2(1-\sigma) + \beta^2 n^2/a^2] - \rho_s h\omega^2 \qquad \text{(A2)}$$

$$S_{23} = E_1[n/a^2 + n\alpha^2\beta^2(2-\sigma) + n^3\beta^2/a^2]$$

$$S_{31} = -S_{13}$$

$$S_{32} = S_{23}$$

$$S_{33} = E_1[1/a^2 + \alpha^4\beta^2 a^2 + 2n^2\alpha^2\beta^2 + n^4\beta^2/a^2] - \rho_s\omega^2 h$$

An axial point force excitation is obtained by setting the right-hand side of the matrix equation to $[F_0 e_n/2\pi a, 0, 0]^T$.

The Interior Spectral Pressure [1]

The interior 'spectral' pressure is given by the formula

$$p_1(r,n,\alpha) = \rho_1\omega^2[\,J_n(\mu_1 r)/\mu_1 J_n'(\mu_1 a)\,]\,\overline{W}(n,\alpha) + A(n,\alpha) \qquad (A3)$$

where $A(n,\alpha)$ is identically zero for point force excitation, and

$$A(n,\alpha) = \pi p_0 e_n[\,J_n(\mu_1 x_0)/J_n'(\mu_1 a)\,]\,[\,J_n(\mu_1 r)Y_n'(\mu_1 a) - Y_n(\mu_1 r)J_n'(\mu_1 a)\,],\ r>x_0$$

$$\qquad (A4)$$

$$A(n,\alpha) = \pi p_0 e_n[\,J_n(\mu_1 r)/J_n'(\mu_1 a)\,]\,[\,J_n(\mu_1 x_0)Y_n'(\mu_1 a) - Y_n(\mu_1 x_0)J_n'(\mu_1 a)\,],\ r<x_0$$

$$\qquad (A5)$$

for a point source excitation.

An alternative to equation (2.2) for the particular case of point source excitation is

$$p_1(r,\emptyset,z) = p_0\exp(ik_1 R_0)/R_0 + (1/2\pi)\sum_{n=0}^{\infty} \cos\,(n\emptyset)\int_{-\infty}^{\infty} b(r,n,\alpha)\exp(i\alpha z)\,d\alpha \qquad (A6)$$

where

$$b(r,n,\alpha) = [\,J_n(\mu_1 r)/J_n'(\mu_1 a)\,]\,[\rho_1\omega^2\overline{W}(n,\alpha)/\mu_1 - \pi i p_0 e_n J_n(\mu_1 x_0)H_n'(\mu_1 a)] \qquad (A7)$$
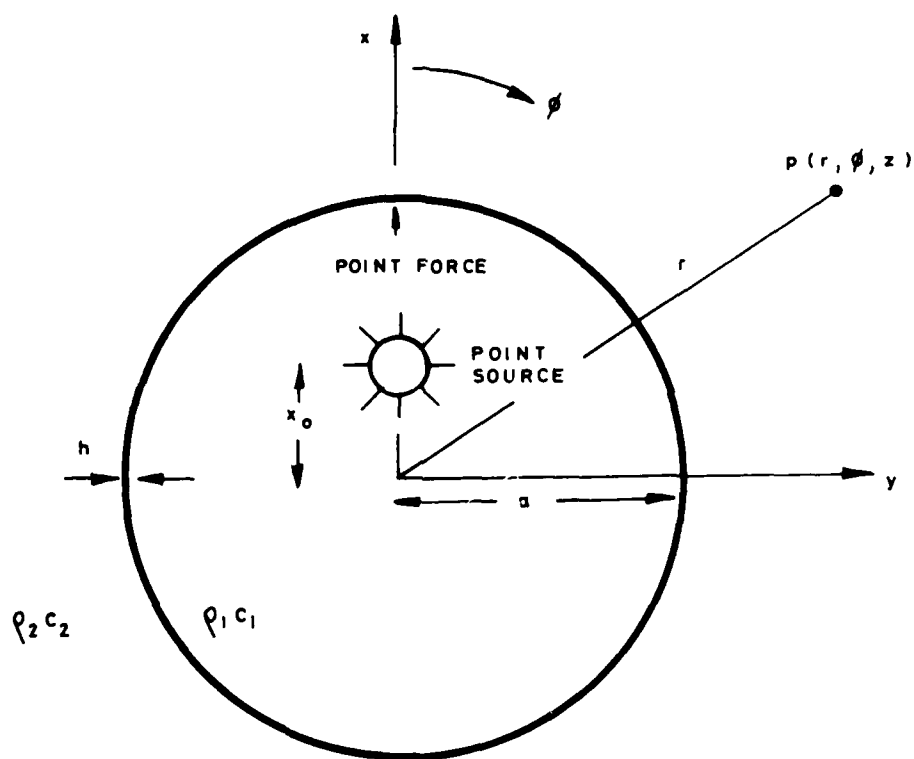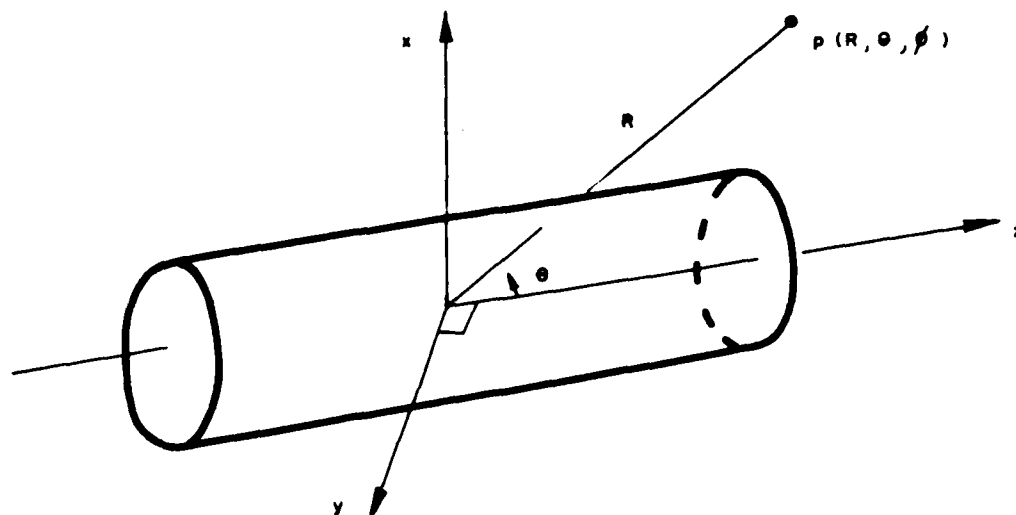
$$x = r . \cos (\phi) \qquad x = R . \sin (\theta) \cos (\phi)$$

$$y = r . \sin (\phi) \qquad y = R . \sin (\theta) \sin (\phi)$$

$$z = z \qquad z = R . \cos (\theta)$$

FIG. 1   GEOMETRY AND COORDINATE SYSTEMS
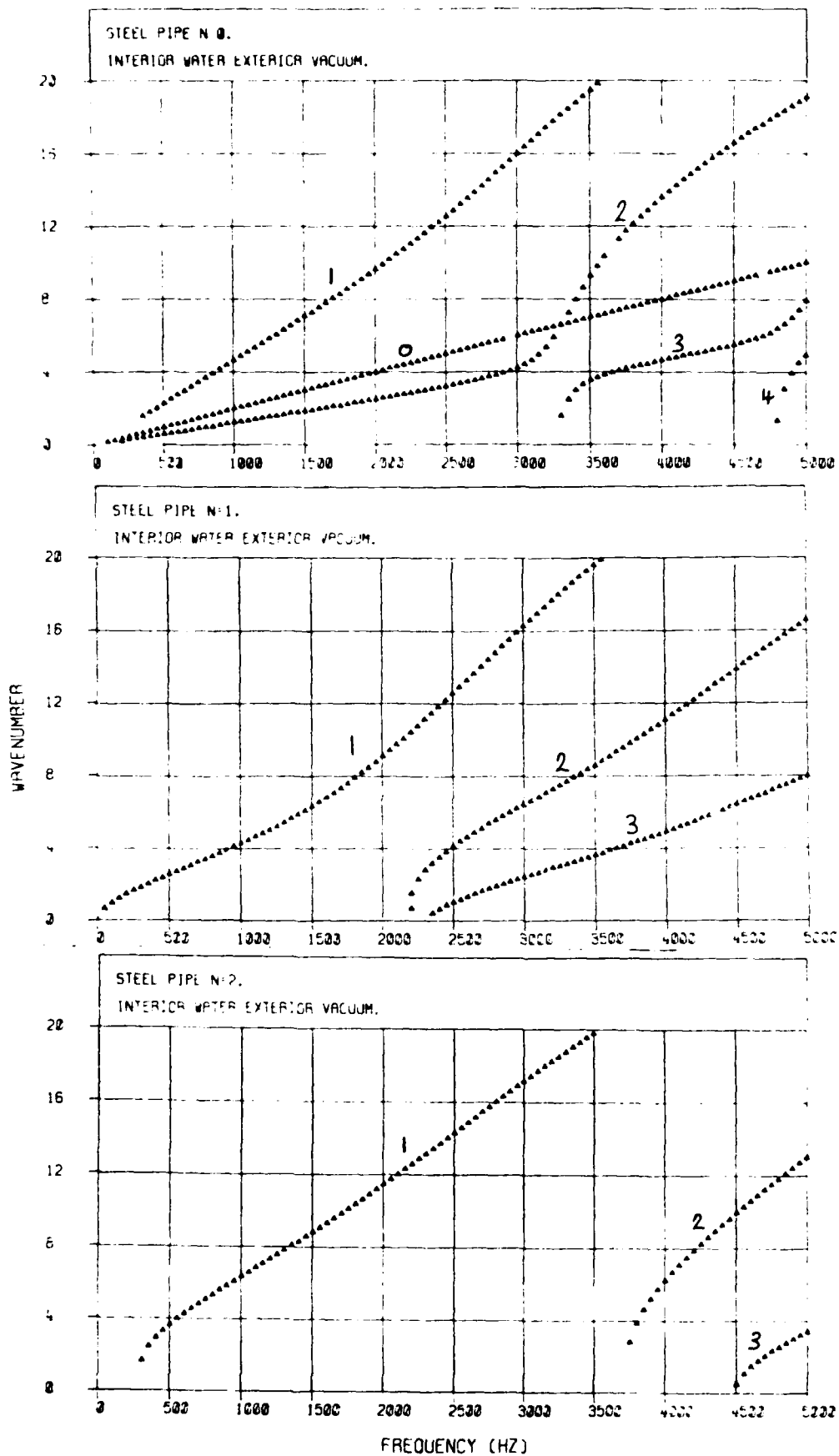
FIG. 2   AXIAL WAVENUMBER VERSUS FREQUENCY.
STEEL PIPE.   INTERIOR WATER.   EXTERIOR VACUUM.

AMTE(N)TM82036
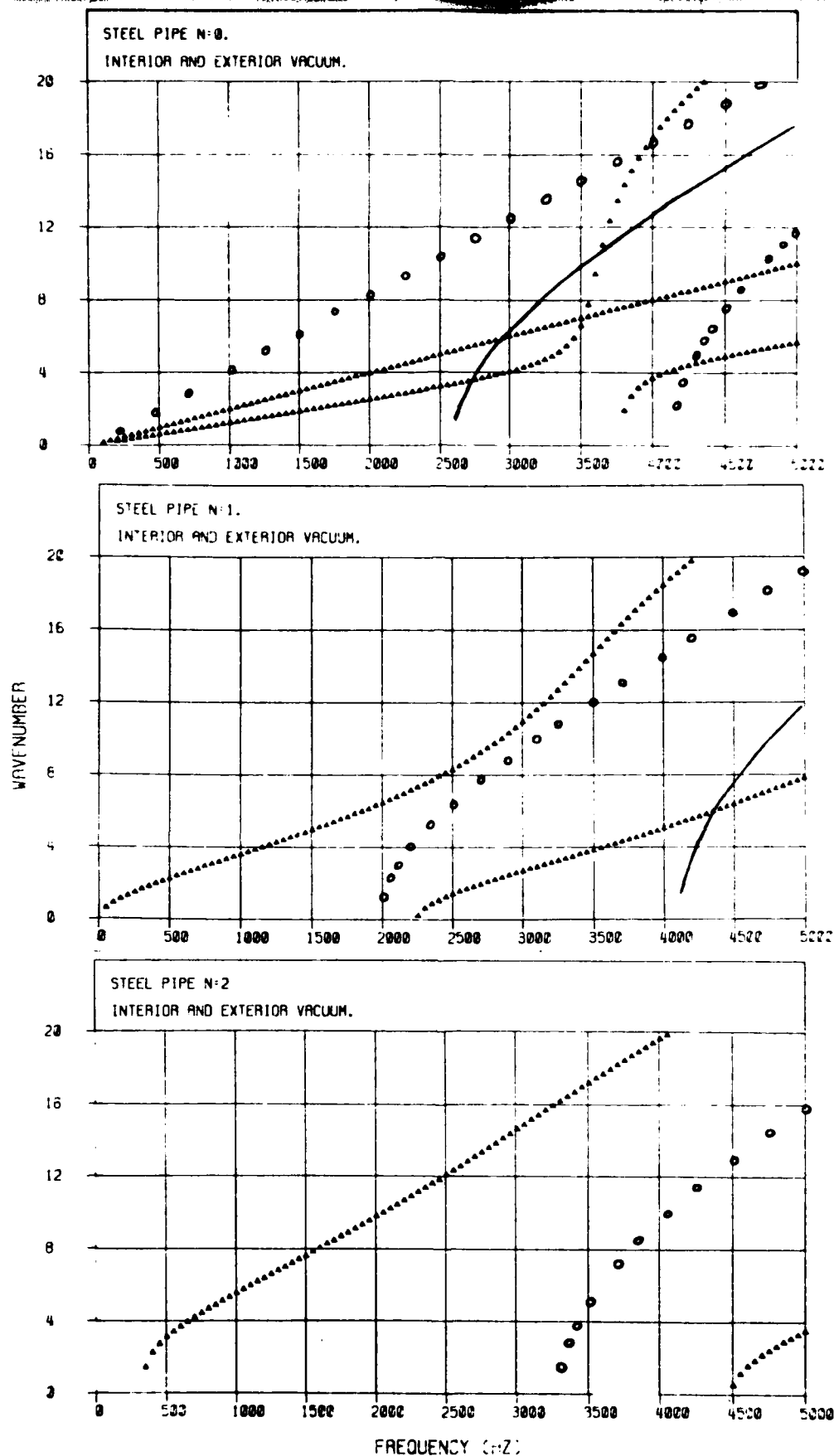
FIG. 3   AXIAL WAVENUMBER VERSUS FREQUENCY.
PIPE IN VACUO ▲▲▲▲
RIGID-WALLED DUCT OF WATER ●●●●
PRESSURE-RELEASE DUCT OF WATER ───
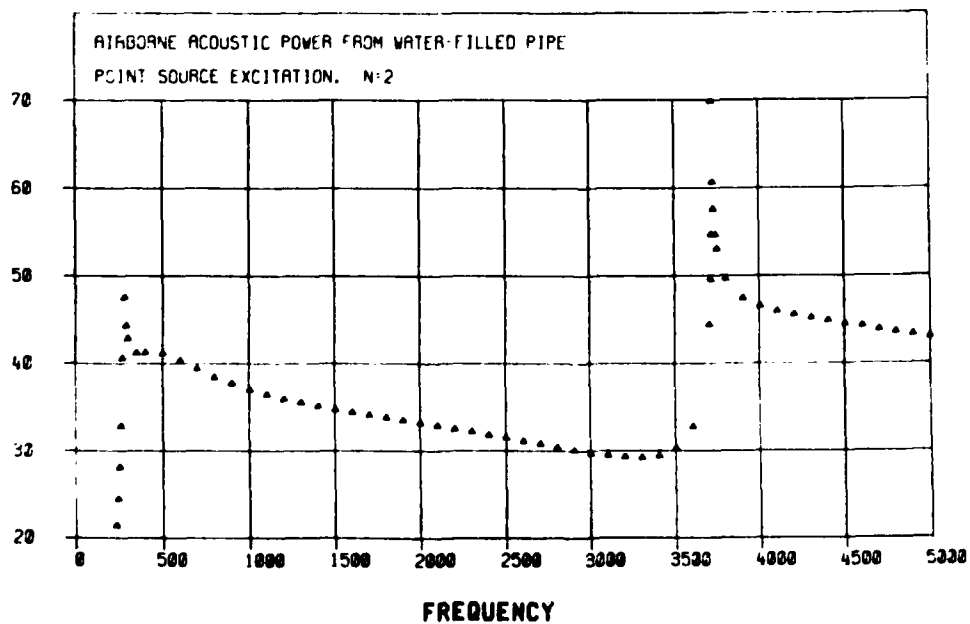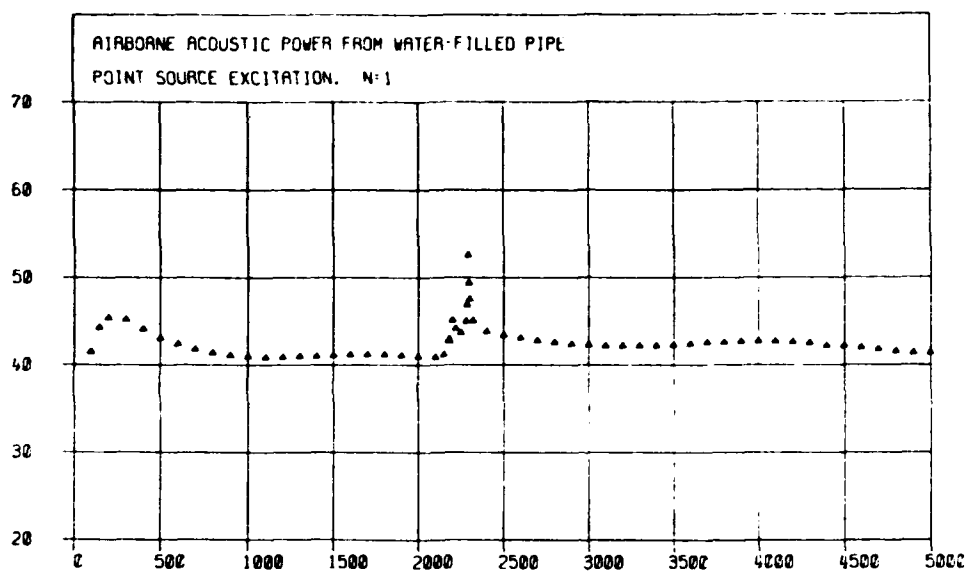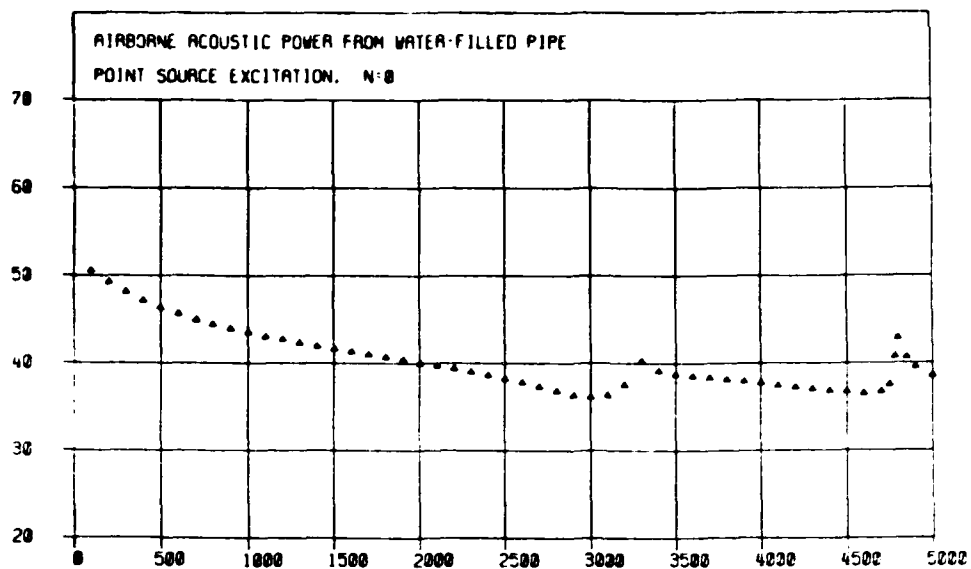
FIG. 4 AIRBORNE ACOUSTIC POWER. SOURCE EXCITATION.

AMTE(N)TM82036
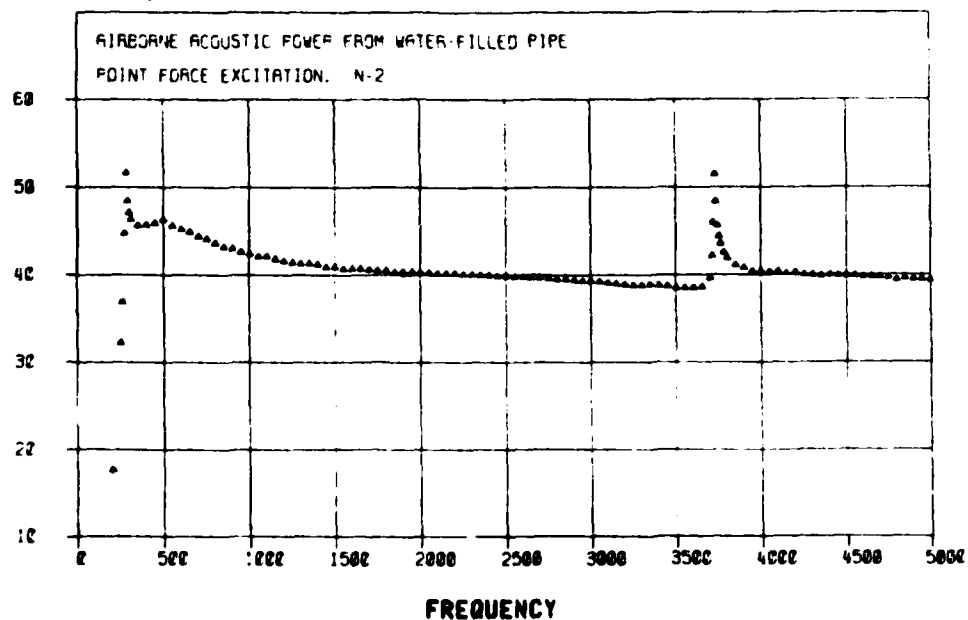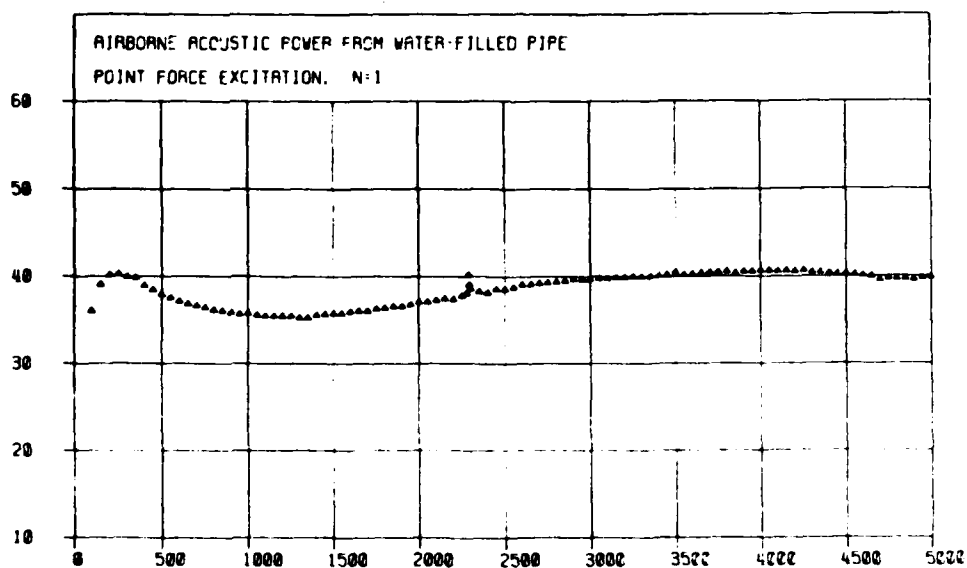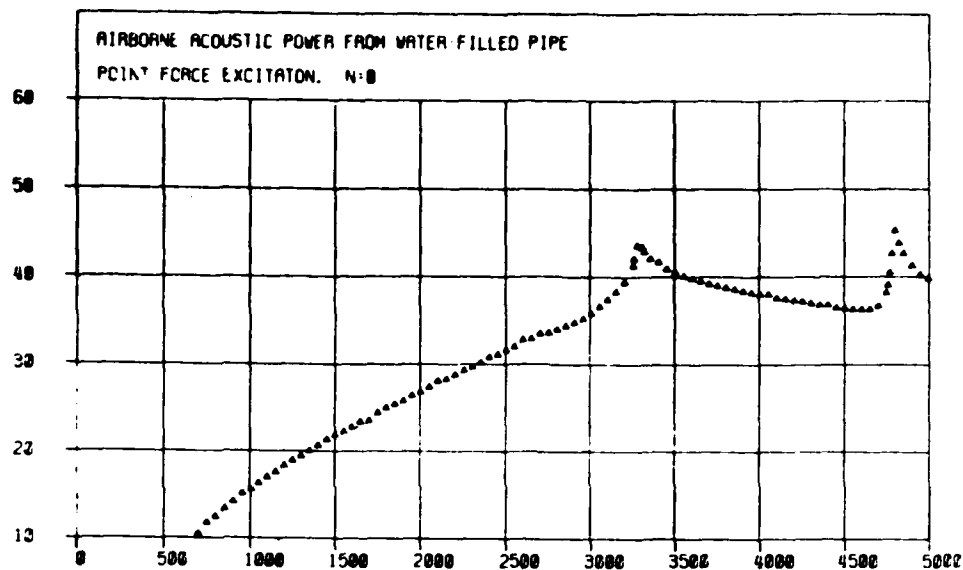
FIG. 5   AIRBORNE ACOUSTIC POWER.   FORCE EXCITATION.
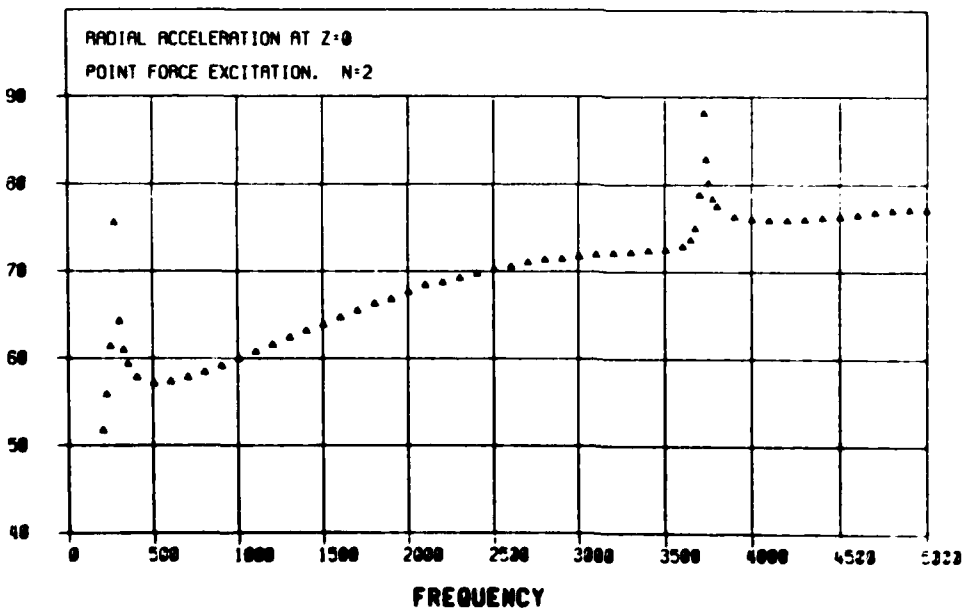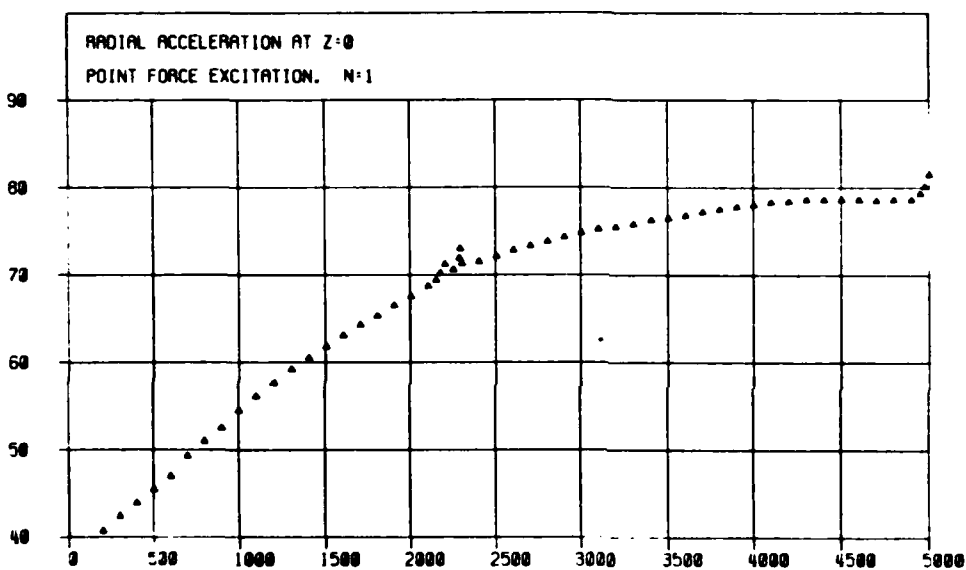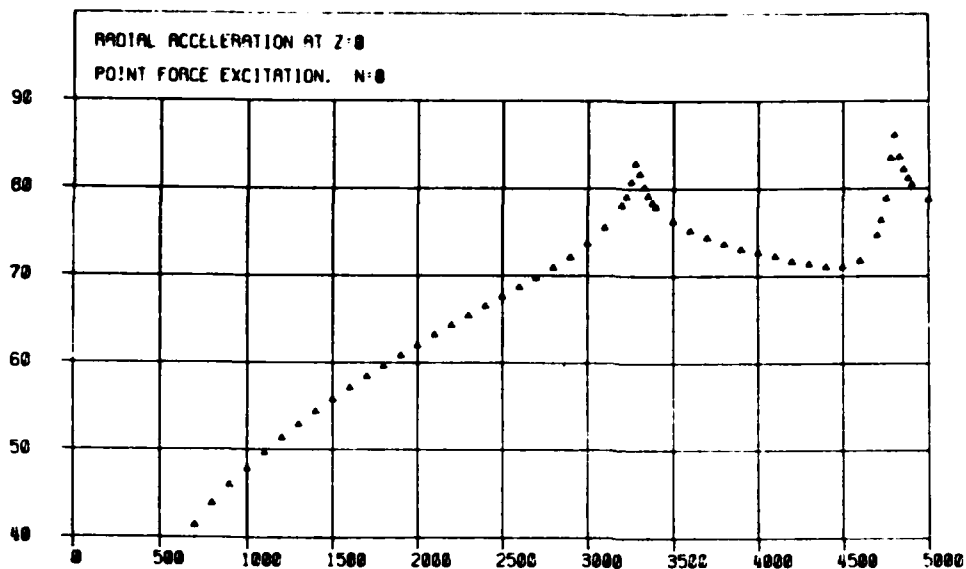
FIG. 6 DRIVE POINT RADIAL ACCELERATION. FORCE EXCITATION.

ANTE(N)TM82036
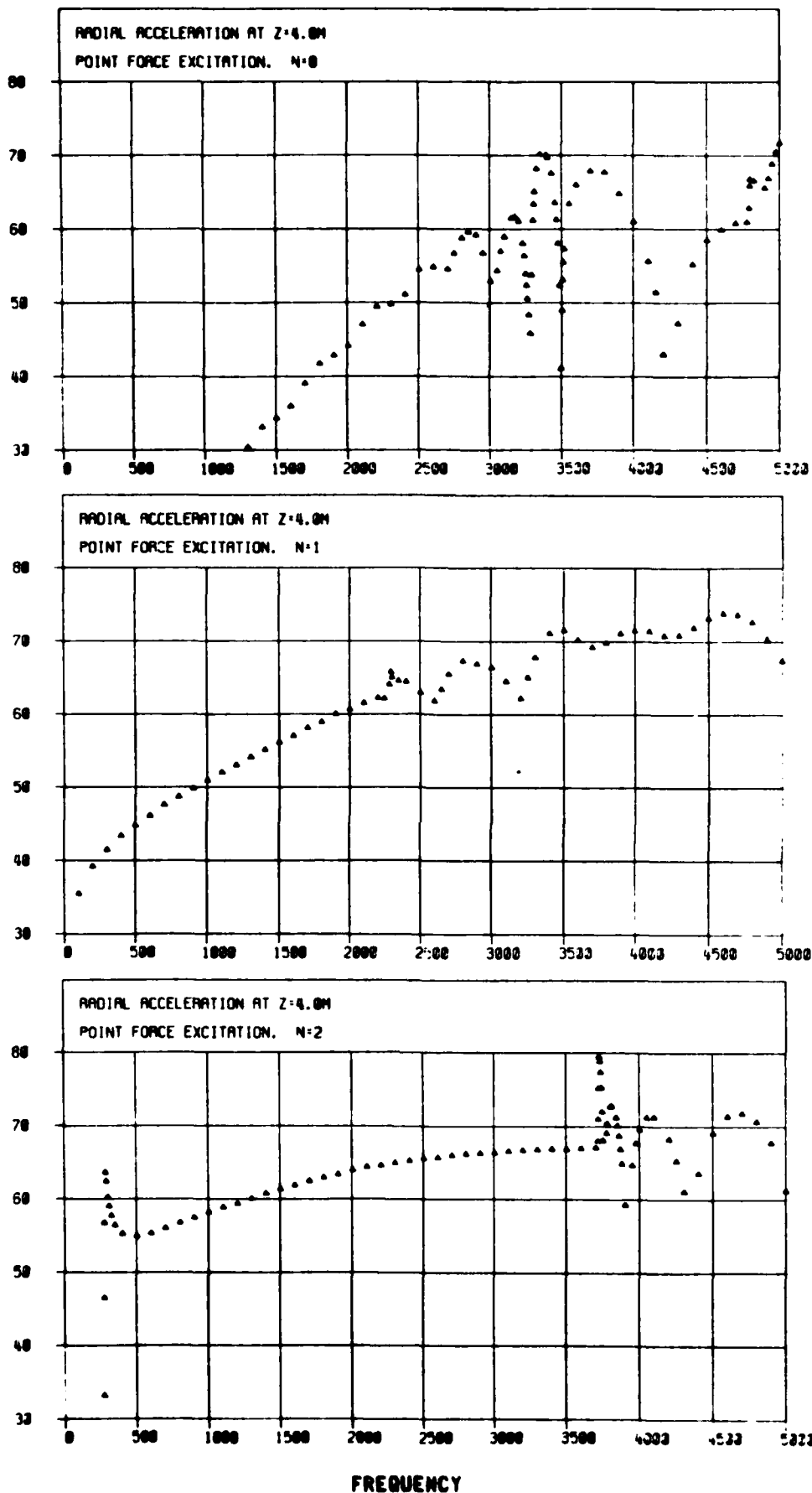
FIG. 7   TRANSFER RADIAL ACCELERATION.   FORCE EXCITATION.
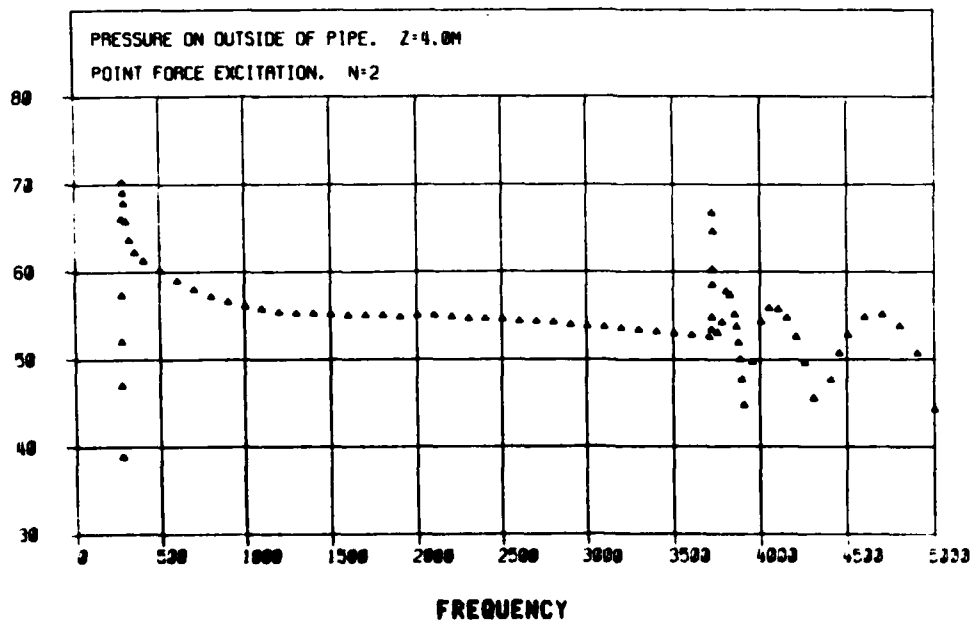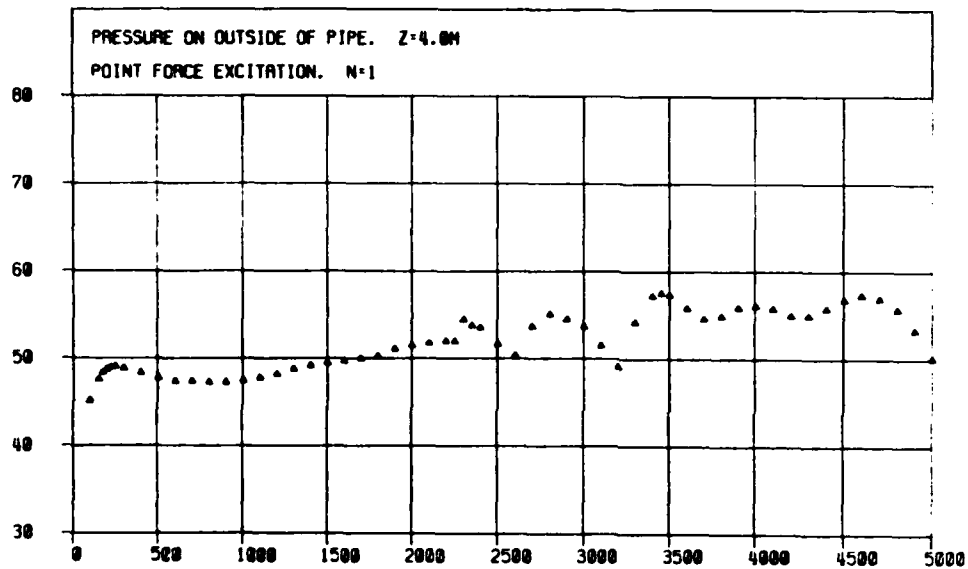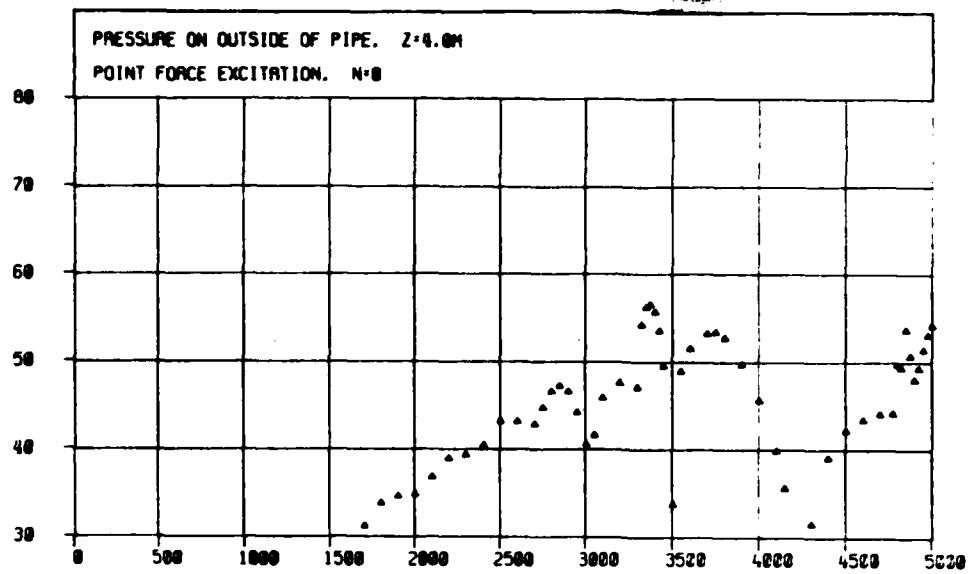
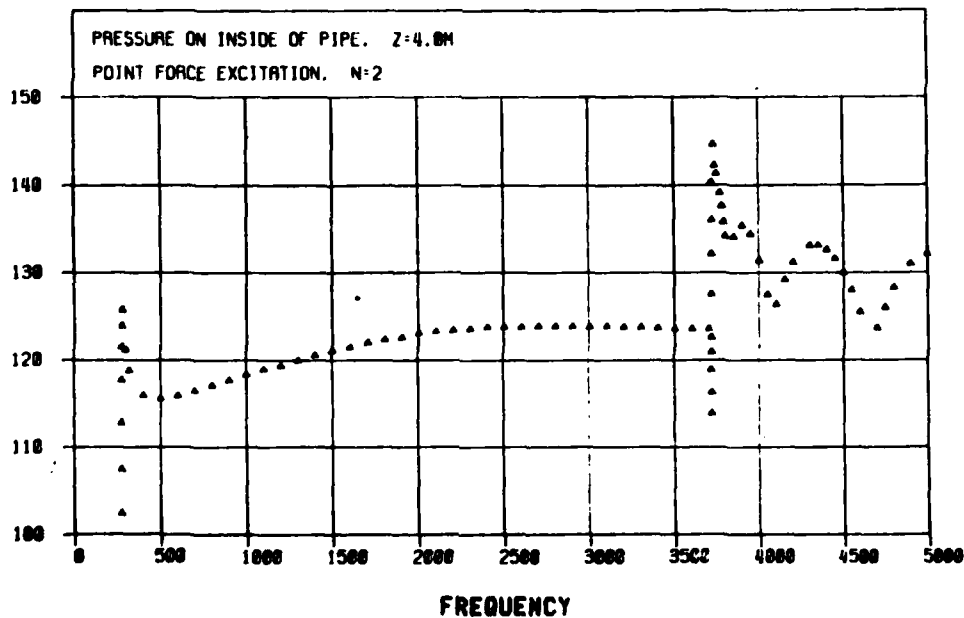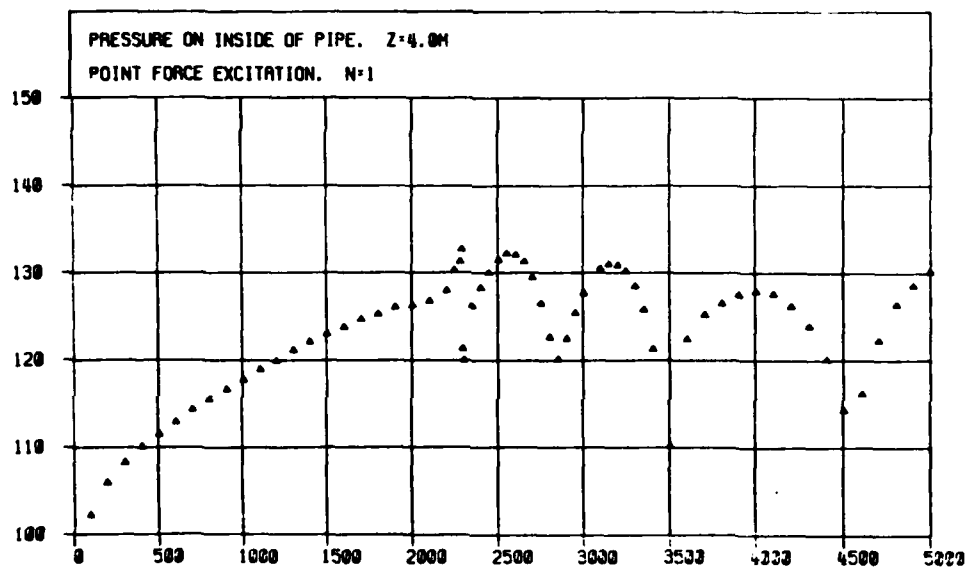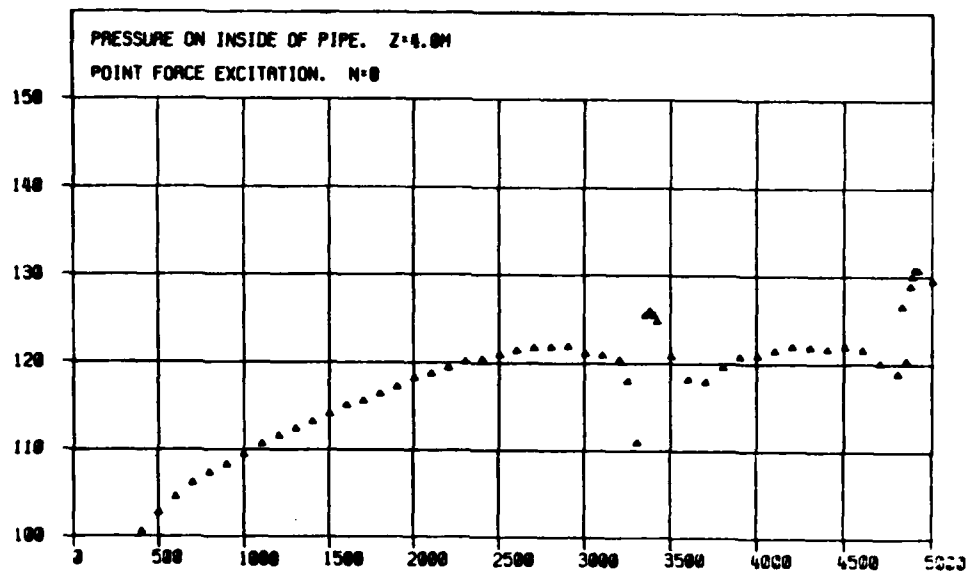FIG. 8 EXTERIOR PRESSURE ON PIPE SURFACE. FORCE EXCITATION.

FIG. 9 INTERIOR PRESSURE ON PIPE SURFACE. FORCE EXCITATION.

FILMED

8-8